Tetrahedron 80 (2021) 131854

Contents lists available at ScienceDirect

Tetrahedron

journal homepage: www.elsevier.com/locate/tet

Synthesis, optical properties and *in vitro* cell viability of novel spiropyrans and their photostationary states

Shiva K. Rastogi [c, *], Zhenze Zhao [c], M. Brenton Gildner [c], Ben A. Shoulders [c], Tara L. Velasquez [c], Madeleine O. Blumenthal [c], Lei Wang [a], Xiaopeng Li [a], Todd W. Hudnall [c], Tania Betancourt [b], Liqin Du [c], William J. Brittain [c]

[a] Department of Chemistry, University of South Florida, Tampa, FL, 33620, USA
[b] Material Science, Engineering and Commercialization Program, 601 University Drive, Texas State University, San Marcos, TX, 78666, USA
[c] Department of Chemistry and Biochemistry, 601 University Drive, Texas State University, San Marcos, TX, 78666, USA

ARTICLE INFO

Article history:
Received 18 October 2020
Received in revised form
1 December 2020
Accepted 2 December 2020
Available online 27 December 2020

Keywords:
Methoxy-spiropyran
UV–Visible
Photostationary state
Anticancer
Photoactivated
Photopharmacology

ABSTRACT

A novel class of spiropyran (SP) was synthesized using a multistep process that involves three key intermediates: (a) diazonium-tetrafluoroborate, (b) hydrazine and (c) indolium iodide. Single crystal X-ray spectroscopy was used to confirm the structure of one of the analogues. The SP analogues were confirmed as being able to isomerize and attain a photostationary state (PSS) upon irradiation with ultraviolet light (UV, 365 nm) in an aqueous environment. UV–visible absorption spectra were recorded to confirm the isomerization properties. The ability of the synthesized compounds to induce growth inhibition of HeLa cervical cancer cells was assessed via the MTT assay after incubation with either the SP or their PSS. The IC_{50} values of two PSS (**PSS-2**, **4**), were observed to be around 14 ± 4 fold lower (26 ± 3 μM) than their corresponding SPs. The most cytotoxic compounds **SP-7** and **PSS-7** showed the lowest IC_{50} values (12 μM). An *in vitro* tubulin polymerization assay showed that **SP-7** and **PSS-7** exhibited the greatest difference in tubulin inhibition relative to unirradiated **SP-1** and **SP-4**.

Published by Elsevier Ltd.

In recent times, stimuli-responsive drug development has attracted considerable interest as a new paradigm to increase the specificity of a drug toward the target diseased cells, increasing the therapeutic effect, and reducing its side-effects. For cancer treatment, in particular, the low specificity of current chemotherapeutic drugs poses dose limitations and causes severe side-effects [1]. To overcome these issues, photopharmacology offers tools to design and develop targeted molecules than can be photoactivated on demand with both spatial and temporal control [2]. Azobenzene analogues, azo-combretastatins A-4 (Azo-CA4) are the examples of photoresponsive anticancer compounds, have been developed recently [3]. Spiropyran (SP), is another photoresponsive and photochromic motif that has been utilized in drug delivery systems for cancer therapy [4], as fluorescence imaging probes of microtubules in living cancer cells [5], and to develop water-soluble photoactivatable cytotoxic moieties [6]. The unique photophysical and photochromic properties of SP inspired us to explore and tailor its basic structure to develop novel cytotoxic photo-pharmacophores.

Structurally, SP comprises of an indole ring and a chromene moiety bound together via a spiro junction (C_{spiro}-O) and oriented perpendicular with respect to one another [7]. SP undergoes thermochromism and photochromism in response to photons, reduction/oxidation, and changes in temperature and pH [8]. In the photochromism process, near ultraviolet light (UV, ~350 nm) and blue (~420 nm) light induce photoisomerization in SP between the colorless SP and colored merocyanine (MC) forms .Scheme- 1b SP analogues are known as molecular photoswitches, used in a broad range of research disciplines such as optical data storage [9], smart materials [10], mechano-chemistry [11], photo induced medicines [12], DNA detection [13], and photo-controlled drug delivery systems for cancer therapy [14].

As previously reported, indole [15], chromene [16], and spiropyran [6] have been shown to possess cytotoxic activity. The unique photo-physical properties of **SP1**-**MC1** isomers and our interest in developing noncytotoxic to toxic photoswitches, prompted us to design and synthesize novel analogues and to investigate their photophysical and biological properties. Specifically, we have developed a new class of **SP1** analogues by tailoring the **SP1**

* Corresponding author.
E-mail addresses: skr55@txstate.edu, rastogisk@gmail.com (S.K. Rastogi).

https://doi.org/10.1016/j.tet.2020.131854
0040-4020/Published by Elsevier Ltd.

structure to include the functional groups common to colchicine and azo-CA4 Fig. 1a on the indole and chromene rings. The PSS of the corresponding SPs were obtained by irradiation in an aqueous environment with UV light (365 nm) to produce equilibrium mixtures of the SP/MC pairs. We then investigated the ability of both SP and PSS forms to induce cancer cell growth inhibition. Finally, we investigated their ability to affect anticancer effects as microtubule inhibitors through an *in vitro* tubulin polymerization assay.

The photochromic properties of **SP1**, **SP6**, and **SP7** in both their SP and PSS states have been well studied in the literature; however, their cancer cell growth inhibition activity and interaction with tubulin has not yet been reported. In this report, the photophysical properties, anti-cancer effect, and the tubulin polymerization inhibition ability of commercially available **SP1**, previously reported compounds **SP6** [17] and **SP7** [18], and four new SPs (**SP2** to **SP5**) Fig. 1b, were investigated in both their SP and photostationary (PSS) states.

The general route for the synthesis of **SP2** to **SP5**, in five steps, is shown in scheme −1. Intermediates **2** and **3** were synthesized as previously reported in the literature [19]. In the first step, *t*-butyl nitrite-mediated nitrogen transfer was carried out on 3,4,5-trimethoxyaniline **1** to give **2** in 92% yield. This was followed by the reduction of **2** to **3** using tin (II) chloride. A solution of **3** in dry dichloromethane (reddish-pink color) was used immediately in the next step without further purification. A solution if **3** in glacial acetic acid was refluxed with 3-Methyl-2-butanone to give **4** ESI (page2-3) and **5** was prepared by the N-methylation of **4** using iodomethane ESI (page3-4). Finally, the novel SPs (**SP2-5**) were synthesized in good yield (65−78%) by condensation of **5** with various *ortho*-hydroxy-benzaldehydes: 2-hydroxy-5-nitrobenzaldehyde **6a**; 2-hydroxybenzaldehyde **6b**; 2-hydroxy-3-methoxybenzaldehyde **6c** and 2-hydroxy-3-ethoxybenzaldehyde **6d** ESI (page4-6).

The intermediates and final compounds were characterized by melting point analysis, nuclear magnetic resonance (NMR) spectroscopy, infra-red (IR) spectroscopy and high-resolution mass spectrometry (HRMS); spectra are in the ESI (page9-33). Additionally, the structure of a representative spiropyran **SP3**, was confirmed unambiguously by single crystal x-ray diffraction studies Fig. 2 and data are listed in the electronic supporting information (ESI; pages 34−37).

The photoisomerization of SPs and MC, leading to the formation of an equilibrium state PSS, was characterized using UV−visible absorption spectrometry Fig. 3. The SP analogues in 5% (v/v) dimethylsulfoxide (DMSO)/phosphate buffered saline (PBS, pH = 7.4) were irradiated with UV light (365 nm). The spectrum of **SP1**, closed-ring isomer shows typical two localized absorption bands. The first band at ~272−296 nm corresponded to the pi to pi-star electronic transition of the indoline moiety, and the ~323−351 nm band was attributed to the chromene moiety. Irradiation of **SP1** with ~365 nm light gives rise to the maximum isomerization into the open-ring isomer **MC1**. This photoisomerization is a first-order process and showed an appearance of a new band at ~480−520 nm [4]. Similar patterns were observed in the UV spectra of **SP2** and **MC2**. However, tailoring of the electron-donating groups and electron-withdrawing groups in **SP3** to **SP7** resulted in a loss of the typical absorption peak at 323−352 nm and, instead the appearance of a band at ~300 nm.

An important feature of the SP-MC system is the equilibrium constant (K_{eq} = [MC/[SP]). The amount of MC in the PSS depends on the electron-donating or electron-withdrawing nature of the substituents on the SP skeleton [20]. As the value of K_{eq} increases, the MC population the in equilibrium increases. Based on the literature reports, we compared and arranged the SPs in increasing order of K_{eq} in non-polar media as $K_{SP7}<K_{SP3}<K_{SP6}<K_{SP5}\sim K_{SP4}<K_{SP1}<K_{SP2}$. However, the quantification of K_{eq} in an aqueous environment is important to correlate the amount of SP and MC, and their effect on biological properties. Hence, we utilized the UV−visible spectra of SP-PSS, from Table- 1 to determine the value of K_{eq}. The absorption intensity at 520 nm was used to represent MC and that at 320 nm to represent SP. The baseline intensity at 630 nm was subtracted from each SP and MC peak value to calculate the amount of SP and MC from its spectrum. The increasing order of K_{eq} for SP was observed as $K_{SP7}<K_{SP6}<K_{SP5}\sim K_{SP3}<K_{SP2}<K_{SP1}<K_{SP4}$ and for PSS was observed as $K_{PSS7}\sim K_{PSS3}<K_{PSS1}<K_{PSS5}<K_{PSS6}<K_{PSS2}<K_{PSS4}$. Based on the K_{eq} order, the concentration of MC was found to be the lowest in the **SP7**-**PSS7** pair and highest in the **SP4**-**PSS4** pair Table- 2.

The exact percentage of the MC in the equilibrium of PSS was quantified using NMR. ^{1}H NMR spectra of SP were recorded in a different aqueous solvent system, such as DMSO-d_6:D_2O (1:9 and 1:1; v/v), CD_3CN:D_2O (3:1; v/v), and CD_3CN:1XPBS (9:1; v/v), but their spectra were unreadable. Only the aqueous mixture of acetone-d_6: D_2O (2:1; v/v) produce suitable to produce NMR spectra for integration quantification. While this solvent mixture is not comparable to cancer cell growth media, we expected that the K_{eq} values of SP and PSS would be comparable in both media. Three to 5 mg of the desired SP compound was dissolved the acetone-d_6: D_2O (2:1; v/v) solvent mixture and the ^{1}H NMR spectra of SP were recorded before and after UV light irradiation. The PSS was produced by irradiation of 365 nm UV light for 30 min on each corresponding SP. The significant differences, in the ^{1}H NMR spectra of **SP1**-**7** and **MC1**-**7** where the downfield shift of aromatic peaks and upfield shift of indole alkyl group peaks in the ^{1}H NMR of their **PSS1**-**7**. The integration ratio of the aromatic-hydrogen peaks of **SP1**-**7** and **MC1**-**7** were used to calculate the percentage of MC in the PSS. Data are reported in Table- 2 and spectra in the ESI (page 38−44).

Chemotherapeutic agents are clinically used for the treatment of

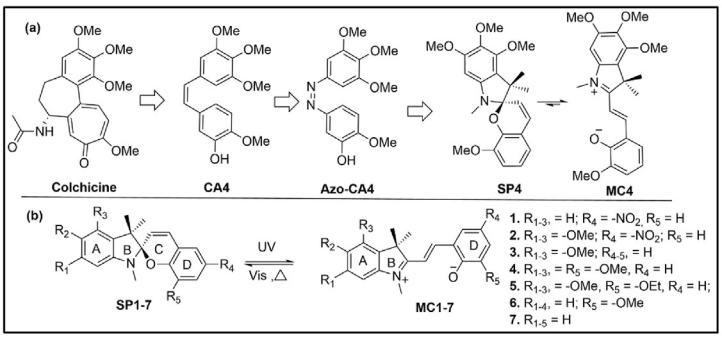

Fig. 1. (**a**) Structures of Colchicine, CA4, Azo-CA4, SP4 and MC4, (**b**) General structure of the SP-MC equilibrium.

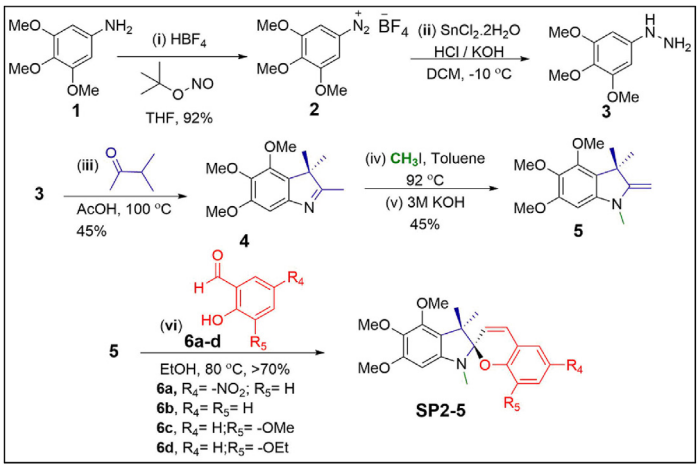

Scheme 1. Synthesis of trimethoxy spiropyrans **SP2-5**.

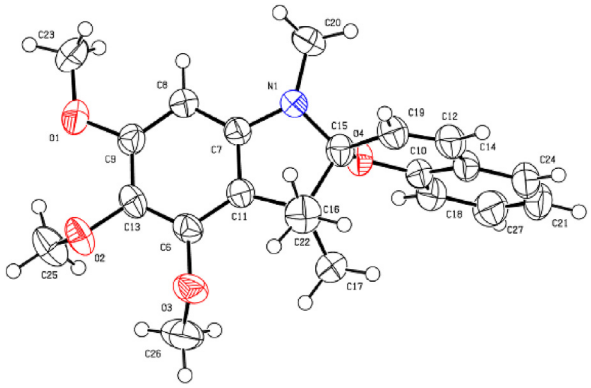

Fig. 2. Crystal structure of SP3.

cancer, but their use can be limited due to serious side effects and toxicity. Hence, researchers are interested in developing effective, non-destructive, and specific new anticancer agents. Photopharmacology offers an opportunity to create more selective cancer-targeting compounds, by applying light to selectively activate photoswitches. Previously we have utilized this elegant approach to develop novel Azo-CA-4 analogues as tubulin polymerization inhibitors [3c].

Herein, we have investigated the HeLa cells growth by incubating with **SP1-7** (prior to UV exposure) or the corresponding **PSS1-7** (UV exposed SP), where HeLa cells were used as a model for human cervical adenocarcinoma cells. The stock solutions of **SP1-7** were prepared in 100%DMSO, then a serial dilution of each compound was prepared in the cell culture medium (DMEM) to incubate HeLa cells, the procedure is reported in ESI (page7). **PSS1-7** were prepared by irradiation with 365 nm light for 30 min in cell growth medium prior to cell incubation. The activity of **SP1-7** and **PSS1-7** on cancer cells was measured with a colorimetric MTT assay Fig. 3. The intensity of color correlates to the viability of remaining HeLa cells; IC_{50} values were determined by curve fitting and statistical analysis Table- 3. The IC_{50} values of **PSS1-5** are lower than the corresponding SPs, while no significant change was observed for those of **PSS6 and PSS7**. More importantly the IC_{50} values of **PSS2, 4, 5** were >4–15 fold lower than their related SPs, which indicates that **PSS-1, 2** and **PSS-4** have potential effects on inhibiting HeLa cell growth. However, **SP7** and **PSS7** showed the greatest inhibition activity on HeLa cell growth with the lowest IC_{50} values. Further, HeLa cells were viable when incubated with a positive control (cell culture medium and without any **SP** or **PSS**) Figure SI-1 and their growth were inhibited after incubating with colchicine, shows a sub-micromolar IC_{50} value Table- 3.

Literature reports show a unique property of **SP1** in an aqueous solution, (i) dramatically higher **MC1** populations in its aqueous **PSS1** solution [21], and (ii) a hydrolytic degradation of **MC1** to its precursor compounds of Fisher's base and the salicaldehyde as above 45 °C and in strong acidic pH conditions [22]. Further the rate of **SP1**-**MC1** interconversion is roughly twice that of the hydrolysis rate of **SP1** compound [23]. Literature show these studies were focused on only 6-nitroSP derivatives, such as **SP1** and **SP2**. As per our investigation, **SP3-7** are predicted to have lower hydrolysis rates and lower K_{eq}. However, we tested the hydrolytic products and starting material (**1**, **2**, **3**, **4**, **5** and *ortho*-hydroxy aldehydes) of **SP1-7** for the growth inhibition of HeLa Cells. But none of them showed cell growth activity and all IC_{50} values were obtained above 100 μM.

In the anti-cancer drug discovery research process, colchicine [24] and combretastatin A-4 (CA-4) [25] have been classified as the ligands that inhibit the polymerization of the mitotic spindle in cancer cells. Therefore, we kept the structure of colchicine and **azo-CA-4** in our mind to design new photoresponsive pharmacophores, we tailor the skeleton of commercial **SP1** and **MC-1**. The preliminary biological evaluation of **SP1-7** and **PSS1-7** indicated significant HeLa cell growth inhibition in the MTT assay. However, to understand and to investigate the possible biomechanism of the novel **SP-PSS** system, we performed an *in vitro* tubulin polymerization assay [26] on **SP1-PSS1**, **SP4-PSS4** and **SP7-PSS7** as per the prescribed procedure for the tubulin polymerization assay kit (Cat. # BK011P) by Cytoskeleton, Inc. ESI (page7). The test results were compared to three different controls: paclitaxel (known microtubule stabilizer), colchicine (known microtubule destabilizer) and DMSO (carrier solvent) Fig. 4. Overall, **SP1**, **SP4** and **SP7** are weak tubulin inhibitors with activities between colchicine and paclitaxel. Little difference was observed between the **SP** and **PSS** of **SP4** and **SP7** while **PSS7** showed the greatest difference in tubulin inhibition assay. Fig. 4 shows the **SP7-PSS7** would be a good hit for further studies. The four hypothesis (i) no substituent on the **SP7** and **PSS7** moieties, (ii) the lowest values of K_{sp}, K_{pss}, (iii) the smallest ligand among the **SP1-6** and **PSS1-6** structures, and (iv) better docking in the colchicine binding site in tubulin protein (PBD: 1SA0) (data not reported here) would be making **SP7** and **PSS7** compound the hit ligand.

Table 1
UV−visible absorption spectra of **SP1-7** recorded at a concentration of 50 μg/mL (0.18−0.12 mM) in a 5% DMSO/1XPBS buffer (pH = 7.4) (v/v). The solutions were exposed to UV light (365 nm) at room temperature (23 °C) for 30 min in a quartz cuvette of 1 cm × 1 cm (width x length); SP = initial spectra before UV irradiation, PSS = spectra after irradiation with UV light (365 nm) for 30 min.

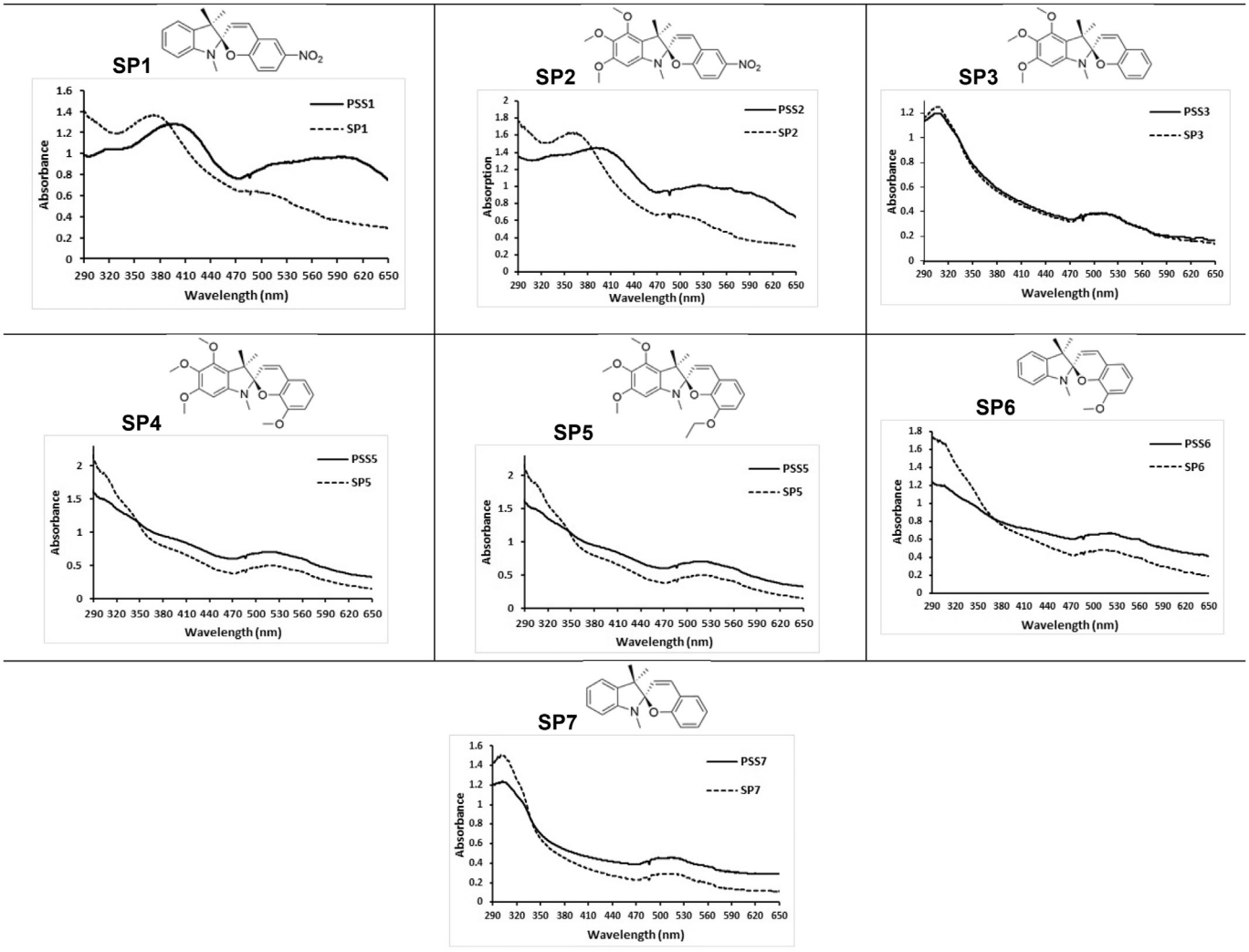

Table-2
Equilibrium constants (K_{sp} and K_{pss}) of SP and PSS solutions at 50 μg/mL (0.18−0.12 mM) in a 5% DMSO/1XPBS buffer (pH = 7.4) (v/v), K_{sp} and K_{pss} were calculated based on the UV−Visible absorption intensity Ksp = MC/SP = $I_{520}-I_{630}/I_{320}-I_{630}$), K_{pss} was calculated from the ratio of the aromatic protons of MC:SP based on peak integration ^{1}H NMR spectra in acetone-d_6/D_2O.

SP or PSS	K_{SP}	K_{PSS}	$K_{PSS/SP}$	MC:SP Ratio in PSS
1	0.31	0.24	0.75	0.25: 1
2	0.25	0.45	1.77	0.45: 1
3	0.23	0.21	0.91	0.2:1
4	0.36	0.52	1.5	0.12:1
5	0.23	0.35	1.51	0.14:1
6	0.21	0.36	1.7	0.05:1
7	0.15	0.2	1.3	0.1:1

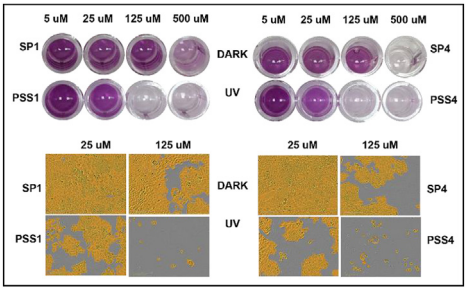

Fig. 3. (Top) MTT assay suspension results in HeLa cells in the presence of 5, 25, 125, and 500 μM of **SP1** and **SP4** in the dark and with UV light. (Bottom) White light microscopic (phase contrast images using a confluence mask of gold color) images of HeLa cells incubated for 72 h with **SP1** and **SP4** in the dark and with UV light.

In conclusion, we have reported the synthesis of four novel spiropyran analogues (**SP2-5**) in five steps using *t*-butyl nitrite mediated nitrogen-transfer and Fisher-indole condensation-cyclization strategies as key steps. X-ray diffraction study was used to confirm the structure of representative **SP3**. Every SP, **SP1-7** was irradiated with UV light (~365 nm) in an aqueous environment to generate its corresponding SP-MC equilibrium, photostationary states (PSS). The formation of PSS, quantification of equilibrium

Table 3
Growth inhibition of HeLa Cells and PSS compositions: [**a**] IC_{50} values for samples without UV treatment (SPs). [**b**] Standard deviation is based on three separate tests; student T-test verified that the difference in IC_{50} is statistically significant for **SP1**-**PSS1** through **SP5**-**PSS5**. [**c**] IC_{50} values for UV irradiated samples (PSSs). [d] Cell culture medium (0.5% DMSO/DMEM).

Entry	IC_{50} [a,b] of SP	IC_{50} [b,c] of PSS	IC_{50}(PSS)/IC_{50}(SP)
1.	>500 μM	30 ± 5 μM	>17
2.	300 ± 70 μM	32 ± 2 μM	10 ± 3
3.	>500 μM	135 ± 9 μM	>4
4.	300 ± 100 μM	23 ± 3 μM	13 ± 5
5.	>500 μM	61 ± 9 μM	>8
6.	160 ± 60 μM	157 ± 6 μM	1.0 ± 0.4
7.	13 ± 3 μM	12.0 ± 0.5 μM	1.0 ± 0.3
8. [d]Blank	ND	ND	
9. Colchicine	0.01 μM		

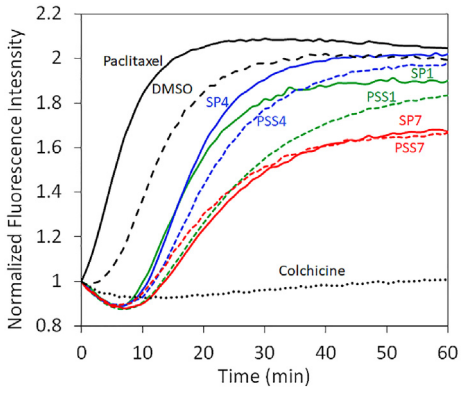

Fig. 4. Effect of **SP1**/**PSS1**, **SP4**/**PSS4** and **SP7**/**PSS7** on *in vitro* tubulin polymerization. Taxol (paclitaxel) (3 μM) promoted microtubule formation relative to 0.05% DMSO. SPs and PSSs (50 μM) in 0.05% DMSO where colchicine (60 μM) completely suppresses tubulin polymerization.

constant and percentage of MC was confirmed and calculate using UV−visible absorption spectra and ^{1}H NMR integration techniques. The cytotoxicity of **SP1**-**7** and **PSS1**-**7** on the HeLa cancer cells was evaluated via the colorimetric MTT assay. **SP1**, **SP2** and **SP4** were found inactive with IC_{50} values of 400 ± 100 μM but their **PSS1**, **PSS2**, and **PSS4** showed HeLa cell growth inhibition with IC_{50} values of 27 ± 3 μM. However, **SP7** and **PSS7** showed the most potent activity with IC_{50} values near 12 μM. **SP7** and **PSS7** were also shown the most activity on tubulin polymerization inhibition. Overall, our research indicates the SP, and their PSS could be an attractive scaffold to develop novel and potential anticancer agents for photopharmacological paradigm. The photoisomerization and bioactivity profiles of **SP1**-**7** and **PSS1**-**7** would be an additional advantage in advance studies of photopharmacology, further the synthetic strategy, describe here could be useful for generating library of novel photoswitchable moieties.

Declaration of competing interest

The authors declare that they have no known competing financial interests or personal relationships that could have appeared to influence the work reported in this paper.

Acknowledgments

We thank the National Science Foundation (PREM center for Interfaces in Materials, DMR-1205670) for financial support of this research. The authors also acknowledge the support of the National Science Foundation for NMR instrumentation (CR1IF:MU0946998 and MRI-0821254).

Appendix A. Supplementary data

Supplementary data to this article can be found online at https://doi.org/10.1016/j.tet.2020.131854.

References

[1] M.M. Lerch, M.J. Hansen, G.M. van Dam, W. Szymanski, B.L. Feringa, Angew. Chem. 55 (2016) 10978.
[2] (a) K. Sanderson, Special to C&EN 96 (2018) 25;
(b) C. Matera, A.M.J. Gomila, N. Camarero, M. Libergoli, C. Soler, P. Gorositza, J. Am. Chem. Soc. 140 (2018) 15764;
(c) W. Szymanski, M.E. Ourailidou, W.A. Velema, F.J. Dekker, B.L. Feringa, Chemistry 21 (2015) 16517.
[3] (a) M. Borowiak, W. Nahaboo, M. Renders, K. Nekolla, P. Jalinot, J. Hasserodt, M. Rehburg, M. Delattre, S. Zahler, A. Vollmar, Dirk Trauner, O. Thorn-Seshold, Cell 162 (2015) 403;
(b) J.E. Sheldon, M.M. Dcona, C.E. Lyons, J.C. Hackett, M.C.T. Hartman, Org. Biomol. Chem. 14 (2016) 40;
(c) S.K. Rastogi, Z. Zhao, S.L. Barrett, S.D. Shelton, M. Zaferani, H.E. Anderson, M.O. Blumenthal, L.R. Jones, L. Wang, X. Li, C.N. Strew, L. Du, W.J. Brittain, Eur. J. Med. Chem. 143 (2018) 1.
[4] S. Barman, J. Das, S. Biswas, T.K. Maiti, N.D.P. Singh, J. Mater. Chem. B 5 (2017) 3940.
[5] H. Zhang, C. Wang, T. Jiang, H. Guo, G. Wang, X. Cai, L. Yang, Y. Zhang, H. Yu, H. Wang, K. Jiang, Anal. Chem. 87 (2015) 5216.
[6] (a) J.R. Nelsson, S. Li, B. Önfelt, J. Andréasson, Chem. Commun. 47 (2011) 11020;
(b) D. Movia, A. Prina-Mello, Y. Volkov, S. Giordani, Chem. Res. Toxicol. 23 (2010) 1459.
[7] R. Klajn, Chem. Soc. Rev. 43 (2014) 148.
[8] (a) L. Kortekaas, W.R. Browne, Chem. Soc. Rev. 48 (2019) 3406;
(b) W.A. Velema, M.J. Hansen, M.M. Lerch, A.J.M. Driessen, W. Szymanski, B.L. Feringa, Bioconjugate Chem. 26 (2015) 2592.
[9] M. Irie, Chem. Rev. 100 (2000) 1683.
[10] (a) L. Wang, Q. Li, Chem. Soc. Rev. 47 (2018) 1044;
(b) J.J. Zhang, J.X. Wang, H. Tian, Mater. Horiz. 1 (2014) 169.
[11] M.H. Barbee, T. Kouznetsova, S.L. Barrett, G.R. Gossweiler, Y. Lin, S.K. Rastogi, W.J. Brittain, S.L. Craig, J. Am. Chem. Soc. 140 (2018) 12746.
[12] (a) J. Broichhagen, J.A. Frank, D. Trauner, Acc. Chem. Res. 48 (2015) 1947;
(b) M.M. Lerch, M.J. Hansen, G.M. van Dam, W. Szymanski, B.L. Feringa, Angew. Chem. Int. Ed. 55 (2016) 10978.
[13] (a) A.A. Ali, M. Kang, R. Kharbash, Y. Kim, BMC Biomed. Engin. 6 (2019) 1;
(b) C. Brieke, A. Heckel, Chem. Eur J. 19 (2013) 15726.
[14] (a) S. Barman, J. Das, S. Biswas, T.K. Maiti, P.N.D. Singh, J. Mater. Chem. B 5 (2017) 3940;
(b) F. Cardano, E.D. Canto, S. Giordani, Dalton Trans. 48 (2019) 15537.
[15] J. Chen, S. Ahn, J. Wang, Y. Lu, J.T. Dalton, D.D. Miller, W. Lin, J. Med. Chem. 55 (2012) 7285.
[16] S.A. Patil, J. Wang, X.S. Li, J. Chen, T.S. Jones, A.S. Ahmed, R. Patil, W.L. Seibel, W. Li, D.D. Miller, Bioorg. Med. Chem. Lett 22 (2012) 4458.
[17] (a) E.I. Balmond, B.K. Tautges, A.L. Faulkner, V.W. Or, B.M. Hodur, J.T. Shaw, A.Y. Louie, J. Org. Chem. 81 (2016) 8744;
(b) J.G. Pargaonkar, S.K. Patil, S.N. Vajekar, Synth. Commun. 48 (2018) 208.
[18] R. Torres, Silvia, S. Vazquez, L. Ana, S. Gonzalez, A. Eduardo, Synth. Commun. 25 (1995) 105.
[19] (a) S. Telitel, A.L. Vallet, D.M. Flanigan, B. Graff, F.M. Savary, T. Rovis, J. Lalevée, J.E. Lacôte, Chem. Eur J. 21 (2015) 13772;
(b) T. Udayabhaskararao, P.K. Kundu, J. Ahrens, R. Klajn, Chem. Phys. Phys. Chem. 17 (2016) 1805;
(c) A. Promchat, P. Rashatasakhon, M. Sukwattanasinitt, J. Hazard Mater. 329 (2017) 255.
[20] N.L. Zaichenko, V.S. Marevtsev, V.D. Arsenov, M.I. Cherkasin, Russ. Chem. Bull. 36 (1986) 1518.
[21] T. Stafforst, D. Hilvert, Chem. Commun. (2009) 287−288.
[22] (a) Y. Shiraishi, M. Itoh, H. Takayuki, Phys. Chem. Chem. Phys. 12 (2010) 13737;
(b) M. Hammarson, J.R. Nilsson, S. Li, T. Beke-Somfai, J. Anderson, J. Phyc. Chem. B 117 (2013) 13561−13571.
[23] D. Movia, A. Prina-Mello, Y. Volkov, S. Giordani, 6-nitroSP refers to 1',3',3'-trimethyl-6nitrospiro[chromene2,2'-indoline] and its derivatives, Chem. Res. Toxicol. 23 (2010) 1459.
[24] (a) B. Bhattacharyya, Med. Res. Rev. 28 (2008) 155e183;
(b) R.L. Margolis, Biochem 19 (1980) 5550.
[25] J.M. Watt, M. Gerdina, The Medicinal and Poisonous Plants of Southern and Eastern Africa, E. & S. Livingston Ltd., Edenburg and London, U.K., 1962.
[26] (a) D. Bonne, C. Heusele, C. Simon, D. Pantaloni, J. Biol. Chem. 260 (1985) 2819;
(b) M.A. Jordan, L. Wilson, Nat. Rev. Canc. 4 (2004) 253.